MOLECULAR SIMULATION STUDY OF DIFFUSION OF METHANE IN A SERIES OF POROUS MATERIALS

[1]Hirvi Shah, [2]Dr.Bhaskarjyoti Borha,
[1]ASSISTANT PROFESSOR, [2]ASSISTANT PROFESSOR
[1]SCIENCE AND HUMENITIES
[1]ADITYA SILVER OAK INSTITUTE OF TECHNOLOGY, AHMEDABAD,INDIA

Abstract : Molecular dynamics simulations were performed to understand the diffusion of methane molecule in different Nano porous metal organic framework (MOFs).Methane is the major component of natural gas and the work presented here is in the perspective of natural gas storage at lowered pressure using sponge like material having high surface area. Diffusion plays major role in storing gas. Once the gas is inside the MOF material it needs to move to the adsorption sites. Moreover, while delivering the gas out of the MOF material at reduced pressure the gas molecules require to move out of the adsorption sites. Higher the diffusion co-efficient the efficient is the material. Diffusion coefficients were calculated at various temperatures – 220 K, 273 K, 298 K, and 350 K. All the diffusion coefficients were obtained using mean square displacement and using the Einstein's relation.

I. INTRODUCTION

The motivation of this project is to understand the diffusion phenomena of hydrocarbons absorbed in porous materials has several industrial applications in petrochemical industries, and it is routine process to separate linear alkenes from branched alkenes. Porous membranes can be used as molecular sieves to separate various hydrocarbon mixtures. Based on the diffusion behavior of various hydrocarbons, one can design innovative separation scheme.

The increasing level of emission of CO_2 in to the atmosphere is getting worrisome and has become a global threat. This dangerously increasing emission is majorly due to burning of coal in power plants and flue gas generated in various industries. Proliferation of automobile using either petrol or diesel as fuel is another large contributor to the total emission. The conventional fuel produces large amount of CO_2 during combustion. Therefore, it has been a constant effort by scientists and engineers to think of an alternate fuel that burns much more cleanly than both petrol and diesel.

Natural gas is indeed a potential alternative because it burns cleaner than conventional fuels. Compressed natural gas (CNG) has been used in automobiles in several countries. There are some disadvantages of using CNG. First of all natural gas is compressed inside the tank at a very high pressure of 220 bar. This requires large compressors and hence makes refueling a tedious task. Moreover, the amount of natural gas required to run a car for a sufficiently long distance demands a large tank.

The placement of the tank in the car creates a major space crunch. Optimization of space and ease of refueling is a major concern in today's world. Therefore, one needs to think of an alternate way of efficient and sufficient storing of natural gas. That requires development of a new design and technology for storing. In recent years, researchers have started working towards achieving the goal of storing methane at ambient temperature and pressure. One of the potential solutions to the problem of storing methane (the major component of natural gas) would be to use some sponge like material which will adsorb large amount of methane

The basic idea is to use these materials inside the tank to store methane instead of using an empty tank. The material filled tank will contain larger amount of methane than an empty tank of same size. Now, the main goal is to design such a material with utmost efficiency. In the recent past, researchers have discovered a new class of material that has well defined micro pores. These materials are crystalline and have specific topologies with structured pores. These materials are called as metal organic framework (MOF)

Over a last decade, metal organic framework (MOF) materials have grabbed great deal of attention as a new addition to the classes of nanoporous materials. MOFs are hybrid materials composed of single metal ions or polynuclear metal clusters linked by organic ligands through strong coordination bonds. Due to these strong coordination bonds, MOFs are crystallographically well defined structures that can keep their permanent porosity and crystal structure after the removal of the guest species used during synthesis, (Yaghi O. M., 2003) MOFs typically have low densities (0.2-1 gm/cm^3), high surface areas (500-4500 m^2/gm), high porosities and reasonable thermal and mechanical stabilities. This combination of properties has made MOFs interesting materials for a wide range of potential applications, including gas storage, gas separation, catalysis and biomedical applications (Eddaoudi M. K., 2002).

MOFs have become attractive alternatives to traditional nano porous materials mostly in gas storage and gas separation since their synthesis can be readily adapted to control pore connectivity, structure and dimension by varying the linkers, ligands and metals in the material. (Düren, 2004) Hundreds of MOF materials with various physical and chemical characteristics have been synthesized to date. (James, 2003) Most of the studies in the literature have focused on a few specific MOF groups such as IRMOFs (isoreticular MOFs) (Eddaoudi M. L., 2000), ZIFs (zeolite imidazolate frameworks) (Park, 2006), CPOs (coordination polymers of Oslo) (Dietzel, 2006), MILs(Materials of the Institute Lavoisier) (Loiseau, 2004), CuBTC (Copper 1,3,5benzenetricarboxylate) (Chui, 1999) and Zn(bdc)(ted)0.5 (Zinc 1,4-benzenedicarboxylicacid-triethylenediamine) (Li, 1998).

For example, Krishna and van Baten studied MOFs and zeolite imidazolate frameworks (ZIFs) for CO_2/CH_4, CH_4/H_2, CO_2/N_2, CO_2/H_2, and hydrocarbon separations. Liu et al. (Liu, 2011) Examined MOFs ability to separate CO_2/H_2 and CH_4/H_2 mixtures. Yang and co-workers investigated separation of CO_2 from flue gases using Cu-BTC. Liu et al. studied separation performances of MOFs and covalent organic frameworks (COFs) for CO_2/CH_4, CH_4/H_2, and CO_2/H_2 mixtures. Goo used molecular simulations for adsorption and separation of CH_4/H_2 mixtures in ZIFs. Jiang's group studied adsorption of CO_2 and CO_2/CH_4 mixtures in ZIFs, bioMOFs, and catenated, metal-exposed, and charged MOFs. Kidskin et al. (Keskin, 1999) examined separation performances of isoreticular MOFs (IRMOFs), bioMOFs, CPOs (coordination polymers of Oslo), ZIFs and COFs for CO_2/CH_4, CH_4/H_2, and CO_2/H_2 mixtures.

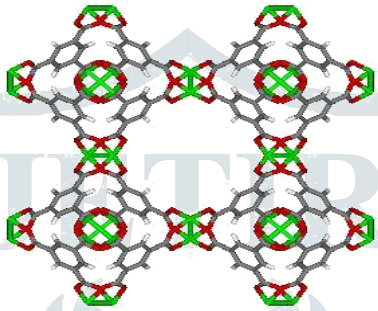

Figure 1 Shows the unit cell structure of one of the most widely studied MOFs, Cu-BTC (also known as HKUST-1) (Keskin, 2012)

II. METHOD AND COMPUTATIONAL DETAIL

In this study, molecular dynamics (MD) simulations were used to compute adsorption and diffusion of CH_4 in MOFs. We have chosen six MOFs having different metal sites, organic linkers, topologies, and pore sizes to represent a variety of MOF properties.

Gas diffusion is an observable consequence of motion of atoms and molecules as a response to external force such as temperature, pressure or concentration change. Molecular dynamics (MD) is a natural method to stimulate the motion and dynamics of atoms and molecules. It is based on Newton's equation of motion. The atoms in the system of interest are considered to be classical particles which follow Newton's equations of motions. The equations of motions are solved using prescribed numerical algorithms available in the literature. There are several techniques to solve the Newton's equations of motion which are based on finite difference methods (Tildesley, 1987). These algorithms have their own pros and cons. The algorithms are chosen based on their efficiency. One of the important factors that have to be taken care of is the energy conservation. The energy of the systems of interest has to be conserved. Some of the algorithms provide good energy conservation and some do not. Efficiency and the degree of conservation decide the algorithm to be used. In the present work we have used the velocity Verlet algorithm (Tildesley, 1987) to solve the equations of motion.

The MD simulations reported in the present work was conducted using LAMMPS program (Plimpton, 1995). This is widely used and freely available program for academicians developed at Sandia National Lab., USA. This program is massively parallelized and can handle systems containing millions of atoms. The most time consuming part of the MD simulation is to calculate the force which is of order N^2. Also, presence of electrostatic interactions might even be time consuming and complicate the computation. These intricacies are handled efficiently using smarter algorithms in LAMMPS.

Every MD simulation requires an initial configuration which contains the positions and velocities of all the atoms in the system of interest. Here, initial configuration of the system obtains using grand canonical Monte Carlo (GCMC) stimulation. The stimulation was performed using RASPA (David Dubbeldam S. C., 2015) program. The initial configuration is then allowed to evolve with respect to time applying the Newton's laws of motion. The system needs to be equilibrated so that the energy is conserved throughout the simulation. During equilibration, the phase space trajectories are not stored until the system has reached equilibration. The phase space trajectory is obtained after a sufficiently large amount of time. The trajectories of each and every particle are then used to calculate the average properties of interest. The equilibrated phase space trajectories are stored at periodic intervals and used them to calculate the mean square displacement. The mean square displacement is then used to calculate the diffusion coefficient using Einstein's equation.

In the present work we have modeled methane as a single spherical bead which has one interaction site. Fifty methane molecules were first adsorbed in the pores of different MOFs. The atoms in the MOF are not included in the time integration of the MD simulation. This leads to a frozen structure of the MOF as a function of time. The interaction between the atoms is very important to model the system. Accurate enough modeling of the interaction potential would provide more physically reliable data which can be

compared to experimental data to a greater precision. We have modeled methane (absorbate)-methane (absorbate), methane (absorbate)-MOF (absorbent), and MOF-MOF interactions using the well-known Lennard-Jones potential

$$U(r_{ij}) = \left(4\varepsilon_{ij}\left[\left(\frac{\sigma_{ij}}{r_{ij}}\right)^{12} - \left(\frac{\sigma_{ij}}{r_{ij}}\right)^{6}\right]\right)$$

Where, σ_{ii} is the size of the atom or the position at which the interaction energy is zero, ε_{ij} is the depth of the interaction potential. r_{ij} is the distance between the i^{th} and j^{th} particle. The potential parameters σ and ε for methane atoms are obtained from the TraPPE force field developed by Siepmann et al. (Siepmann, 1998) On the other hand, the parameters for the
MOF atoms were obtained from the DREIDING force field (S. L. Mayo, 1990). As an example, the potential parameters which are used in this stimulation are given in table-2

Table 1 Potential parameters are used for adsorbate molecules in MD simulations.

Atoms/molecules	**Energy parameter(ϵ)** **kJ/mol**	**Size parameter(σ)** **(Å)**
C-C	0.103602	3.43085
H-H	0.0439977	2.57113
O-O	0.05999	3.11814
Zn-Zn	0.0048802	2.46155
Zr-Zr	0.068996	2.78316
Cu-Cu	0.00499	3.11369
CH_4-CH_4	0.294076	3.73

Since, the interaction between absorbate-absorbent has taken in order to get the values of Ɛ and σ use the given formula below, which known as Lorentz-Berthelot rule.

$$\sigma_{ij} = \frac{\sigma_{ii} + \sigma_{jj}}{2}$$

(Lorentz, 1881).

$$\epsilon_{ij} = \sqrt{\epsilon_{ii}\epsilon_{jj}}$$ (Berthelot,1898)

The simulations in the present work were performed at various temperatures namely, 220 K, 273K, 298 K, and 350 K. All the simulations were done in NVE ensemble at a given temperatures. The system was equilibrated for initial 1 ns run and then another 1 ns run was made during which the position and velocities of each and every atom were stored at an interval of 1 ps. An integration time step of 1 fs was sufficient to obtain good energy conservation. The force calculation was done by using a cut off radius of 14 Å which reduces the amount of computations. Periodic boundary conditions were employed in all the three directions in order to get rid of the surface effects.

After defining all the parameters, run the MD stimulation. Newton's equation is integrated and the position and velocities are obtained. It is done for all the six MOFs where each MOF are stimulated at four different temperatures (220K, 273K, 298K &350K).

2.1 Crystallographic details of the MOFs

Structural information of MOFs having cubic structure (α=β=γ=90˚).

Table 2 The structural details of the MOFs.

Materials	Cell volume	Symmetry space group name hall	Symmetry Cell Setting	Symmetry space Group name H-M	Lattice Parameter a=b=c(Å)
Cu-BTC	18280.8	-F 4 2 3	Cubic	F m -3 m	41.401
IRMOF-1	17237.5	-F 4 2 3	Cubic	F m -3 m	26.343
MOF-205	27964.4	P 1	Triclinic	P 1	25.832
IRMOF-10	40285.5	-F 4 2 3	Cubic	F m -3 m	42.796
PCN-61	78379.7	-F 4 2 3	Cubic	F m -3 m	30.353
UIO-66	8870.26	P 1	Triclinic	P 1	34.281

III. RESULTS AND DISCUSSION

3.1 STRUCTURAL CHARACTERIZATION OF MOFS:

Different structural properties of all chosen MOFs have been calculated. Structural properties such as void fraction(V_F),largest pore diameter(LPD),dominate pore diameter(DPD),pore limiting diameter(PLD),gravimetric surface area(S_G),volumetric surface area(S_V) are obtain using different algorithms available in the literature.in Table-3,all the structural properties of different MOFs consider in this work are describe.

Table 3 Contain the information of MOFs parameter**.**

Materials	V_F (Å)	DPD (Å)	LPD (Å)	PLD (Å)	S_G (m^2/g)	S_V (m^2/cm^3)
UIO-66	0.49	6.022	6.02	2.14	799.65	997.84
Cu-BTC	0.74	10.5	12.47	4.98	2071.11	1828.70
IRMOF-1	0.8	14.42	14.42	10.98	3494.60	2073.68
PCN-61	0.82	6.66	17.94	3.06	3666.09	2055.72
MOF-205	0.87	21.9	21.90	8.06	4675.78	1786.43
IRMOF-10	0.88	19.9	19.90	16.41	4911.69	1616.84

Void fraction (V_F) is a measure of the void (i.e. "empty") spaces in a material, and is a fraction of the volume of voids over the total volume, between 0 and 1, or as a percentage between 0 and 100%. Strictly speaking, some tests measure the "accessible void," the total amount of void space accessible from the surface.

Dominating pore diameter (DPD) is defined as the dominating largest opening along the pore. This quantity in our case is similar to largest pore diameter. Pore limiting diameter (PLD) is defined as the smallest opening along the pore that a molecule needs to cross in order to diffuse through the given material. This quantity is also known as the largest free sphere. Largest pore diameter (LPD) is defined as the largest opening along the pore. This quantity is also known as largest included sphere Surface area is define as the surface area that absorbate molecule can access inside the pores of a material. Volumetric surface area (S_V) is the surface area to volume ratio means the amount of methane absorbed per unit volume of MOF sample. Gravimetric surface area (S_G) is the surface area to mass ratio means the amount of methane absorbed per unit mass of the MOF sample.

3. 2 ESTIMATION OF DIFFUSION CO-EFFICIENT:

Phase space trajectories of the methane molecules were generated after running the MD simulation for 1 ns equilibration and 1 ns production. These stored trajectories were then used to calculate the mean square displacements which provide the diffusion coefficients. In order to get diffusion coefficient, we have calculated the mean square displacements (MSDs) with respect to time. We plot the MSD as function of a time. Least square fitting is performed on the MSDs to estimate the diffusion coefficient. The Einstein relation is used to get the discussion coefficient.

$$D_S = \lim_{t\to\infty} \frac{1}{6t} < \Sigma [r_{il}(t) - r_{il}(t)]^2 N_{il=1} >$$

Diffusion coefficient obtained from the MSDs for all the MOFs and at all the temperatures are listed in Table-4 & MSDs are shown in Figure-2.It is clearly seen from the fig that the MSDs are quite linear w.r.t time. This indicates good statistical estimation.

Table 4 The diffusion co-efficient of respected MOFs at different temperature has been given.

Materials	**T=220K**	**T=273K**	**T=298K**	**T=350**
UIO-66	12.45083	14.45167	15.46167	18.2733
CU-BTC	8.751667	11.05183	11.19467	10.57783
IRMOF-1	9.6385	12.4045	12.4245	15.44133
PCN-61	18.615	24.45167	25.74667	26.72833
MOF-205	13.63367	17.39667	17.50333	19.33833
IRMOF-10	11.67617	18.95667	20.81333	22.1833

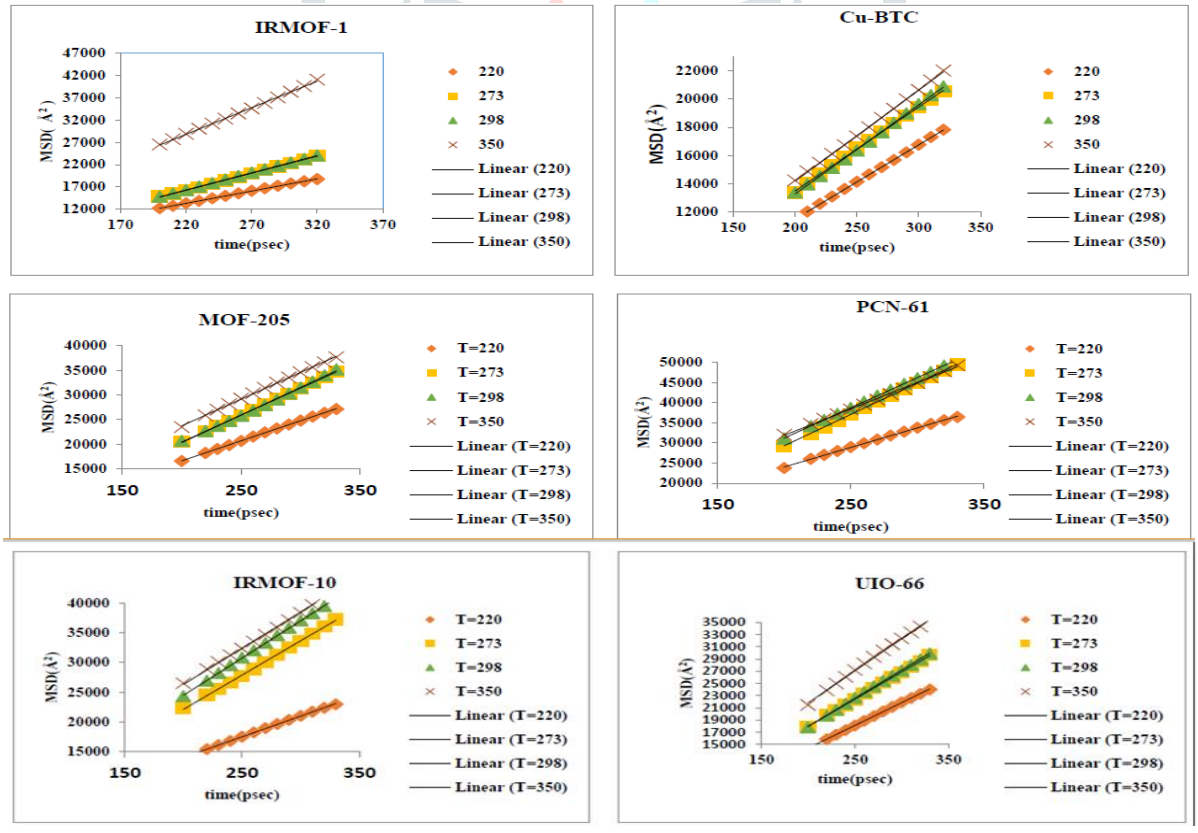

Figure 2 Mean square displacements as a function of time for all the six MOFs

3. 3STRUCTURAL PROPERTIES CORRELATION:

3.3.1 Correlations between diffusion coefficient and surface area (gravimetric & volumetric) 1Correlations between diffusion coefficient and surface area (gravimetric & volumetric)

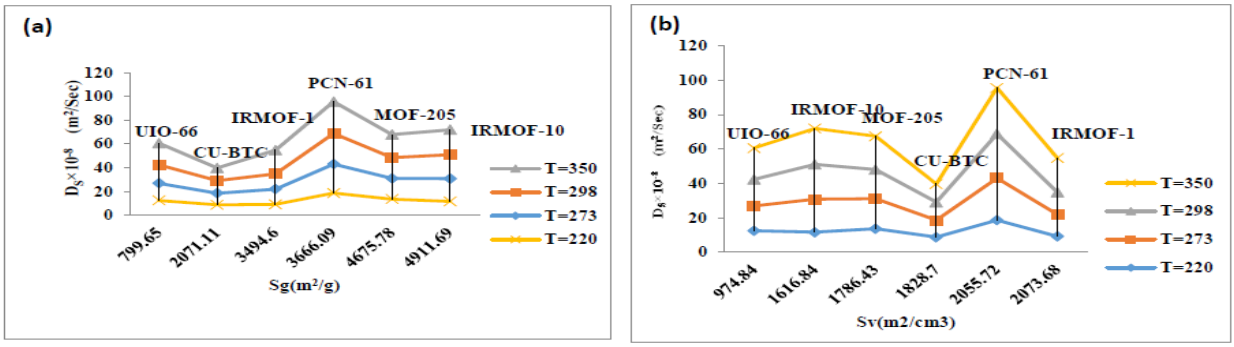

Figure 3 (a) Diffusion coefficient as a function of volumetric surface area and (b) Diffusion coefficient as a function of volumetric surface area

Self-diffusion coefficients are plotted as function of surface area of all the MOFs, as shown in Figure-3.The diffusivity initially decreases as function of surface area and after reaching a minmum.it start increasing to maximum. Further increase of surface area, reduces the diffusion coefficient. This trend is observed for all the temprature.it is clearly observe that PCN-61 has the highest diffusion coefficient than Cu-BTC has the lowest. This non-monotonic behavior of diffusivity can be explained in terms of the pore sizes of concerned MOF, a possible explanation is followed from the correlations of diffusivity as function of pore limiting diameter (PLD).

Table 5 The percentage error between the PCN-61 and Cu-BTC.

Temperature(K)	Percentage difference (%)
220	72.081
273	85.6
298	83.58
350	86.67

3.3. 2CORRELATION BETWEEN DIFFUSION COEFFICIENT AND PORE SIZE:

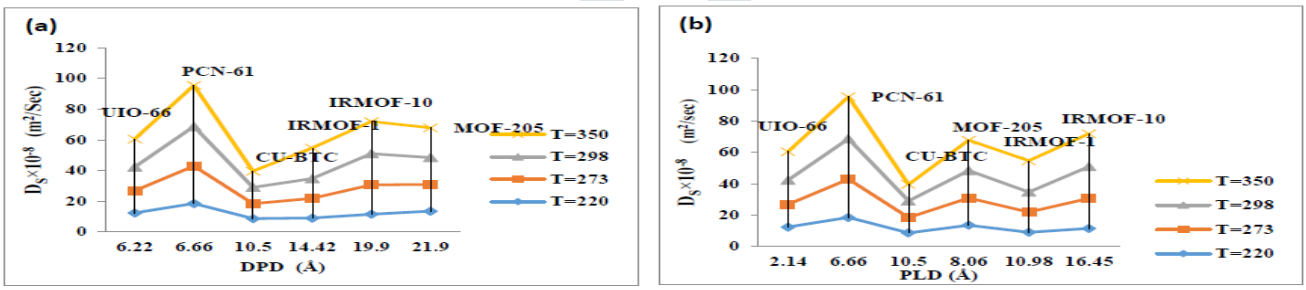

Figure 4 (a) Diffusion coefficient as a function of dominant pore diameter (DPD), (b) Diffusion coefficient as a function of pore limiting diameter (PLD).

The pore size distribution to all the MOFs are calculated using simple Widom insertion method from the pore size distributions. We obtained the PLD connecting to bigger cages and diameters of dominating pore. Correlation of the diffusion coefficients w.r.t PLD and DPD are shown in Figure-4.the diffusivity of methane in PCN-61 is largest as seen in the previous Figure-3.This behavior of diffusion coefficient can be explained as follows. The size of methane is around 4 Å and pore limiting diameter of PCN-61 is 6.6 Å **.**This indicates the size of methane is comparable to the PLD of PCN-61, therefore methane molecules could hop from one pore to another pore by crossing the bottleneck through its center. During this motion the forces acting on methane molecule by MOF atoms are more or less equal and opposite. Thus, net force acting on methane molecule is close to zero making its motion facile. When the PLD or diameter of bottleneck is much larger then methane molecules crosses the bottleneck by crowing along the surfaces of MOFs. These way methane molecules have a net force of significant value due to the MOF atoms. Therefore the methane molecules are bound to the surface of MOF and hence its diffusion coefficient is much lower.

In order to investigate non-monotonic behavior of diffusion coefficient as a function of pore sizes and surface area, we have obtained the activation energy of all MOFs.

3. 4 ACTIVATION ENERGY:

The diffusion coefficients at four different temperatures were obtained as described in Table-4.the diffusion coefficient are plotted as function of temperature as shown in the Figure-5.

The logarithm of diffusion coefficient as a function of inverse of temperature, shows an Erroneous relation given by

$$D_s = D_0 \exp(-E/RT)$$

Where R=gas constant

T=temperature

Least square fitting were performed to obtain the slope of erroneous plot in Figure-6.the activation energy were obtained from the erroneous plots are listed in table-6,from the fig-5.it is clearly seen that activation energy for PCN-61 is largest for Cu-BTC it is the least.

In porous material like zeolites and MOFs the activation energy is related to the potential energy surface inside this material the activation energy indicates the height of potential energy barrier faced by the guest molecule, while moving inside the porous material. Therefore activation energy should be inversely related to the diffusion coefficient .when the activation energy are higher the diffusion coefficient proportionally lower, and visa-versa.in the present work we observed that the different coefficient of PCN-61 is largest. Therefore activation energy of methane in PCN-61 should be expectedly low.in the center PCn-61 has highest activation energy. Similarly Cu-BTC whose diffusion coefficient is the least, should have the highest activation energy. Our observation contradicts with this general correlation of diffusion coefficient with activation n energy. This phenomenon is surprising and out of our understanding at present status of work.

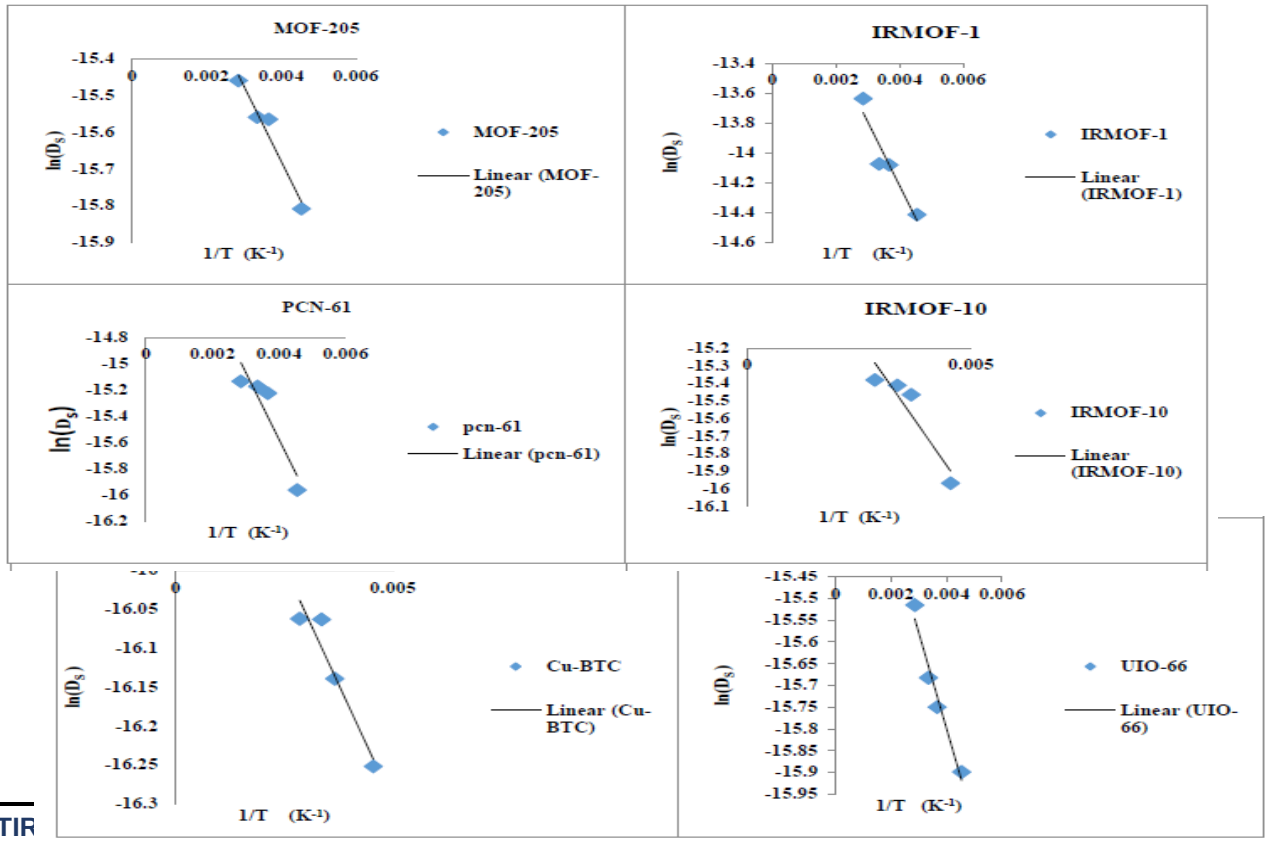

Figure 5 ln (Ds) as a function of 1/T graphs for different MOFs are shown which come nearly linear

Table 6 The energy in kJ/mol is given for all six MOFs

Material	**Energy (kJ/mol)**
Cu-BTC	0.24016869
IRMOF-1	0.52850226
IRMOF-10	0.78534188
MOF-205	0.40791123
PCN-61	1.02062255
UIO-66	0.43771623

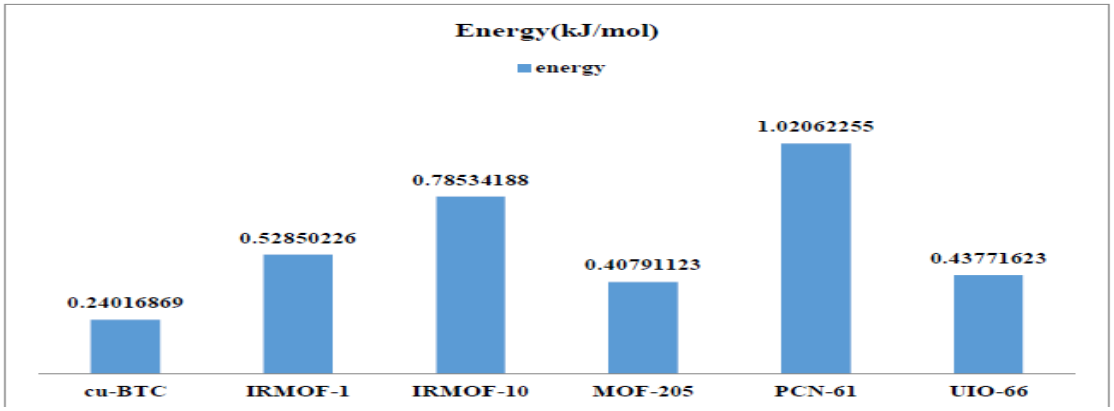

Figure 6 Activation energy for different MOFs material

PCN-61 the activation energy is high and for Cu-BTC the activation energy is low.

IV. CONCLUSIONS

We have carried out molecular dynamics simulation to understand the diffusion of methane in different MOFs as a function of temperatures, and diffusion coefficients were calculated using the mean square displacements of the methane molecules. We applied Einstein's relation to calculate the diffusion coefficients from the slope of the mean square displacements. We found that as temperature increases the diffusion coefficient respectively increases for all the MOFs. From the data we conclude that PCN-61 has highest diffusion co-efficient and Cu-BTC has lowest diffusion co-efficient. According to kinetic theory, higher the diffusion co-efficient lower the activation energy, but in our work the PCN-61 has high diffusion co-efficient as well as high activation energy which contradict the kinetic theory. A detail work would require to understand the contradictions that we observe concerning diffusion coefficient and activation energy.

FIGURES

TABLES

V. ACKNOWLEDGMENT

I would like to thank my supervisor Dr. Bhaskarjyoti Borah for his constant support and encouragement, I would also like to mention my sincere gratitude to Dr. R V Upadhyay (Dean, P.D PATEL INSTITUTE OF APPLIED SCIENCE) and my colleagues for their help and support.

VI. REFERENCES

1) B. Borah, H. Z. (2015). Diffusion of methane and other alkanes in metal-organic frameworks for natural gas storage. Chem. Eng. Sci., 135-143.
2) Baten, R. K. (2008). Insights into diffusion of gases in zeolites gained from molecular dynamics simulations. Micropor. Mesopor. Mater., 91-108.
3) C. Chmelik, J. K. (2009). Adosption and diffusion of alkanes in CuBTC crystals investigated using infra-red microscopy and molecular simulations. Micropor. Mesopor. Mater., 22-32.
4) C. L. J. Rowsell, a. O. (2004). Metal-organic frameworks: a new class of porous materials. Micropor. Mesopor. Mater., 3-14.
5) Chui, S. S. (1999). A. Science, 283, 1148-1150.
6) D. C. Ford, D. D. (2009). The effect of framework flexibility on diffusion of small molecules in the metal organic framework IRMOF-1. Diffusion fundamentals, (pp. 459-466). Leipzig, Germany.
7) D. C. Ford, D. D. (2012). Self-diffusion of chain molecules in the metal-organic framework IRMOF-1: Simulation and experiment. J. Phys. Chem. Lett., 930-933.
8) D. Dubbeldam, R. Q. (2007). Recent developments in the molecular modeling of diffusion in nanoporous materials. Mol. Simulat., 305-325.
9) David Dubbeldam, S. C. (2015). RASPA 1.9.15: Molecular Software Package for Adsorption and. molecular stimulation.
10) Dietzel, P. D. (2006). Hydrogen. Chem. Commun.,, 961.
11) Düren, T. S. (2004). Design of New Materials for. Langmuir, 20, 2683-2689.
12) Eddaoudi, M. K. (2002). Systematic Design of Pore Size and Functionality in Isoreticular MOFs and Their. Science, 295, 469-472.
13) Eddaoudi, M. L. (2000). Highly Porous and Stable Metal-Organic. J. Am. Chem. Soc, 122, 1391-1397.
14) F. Stallmach, S. G. (2006). NMR studies on the diffusion of hydrocarbons on the metal-organic framework materials MOF-5. Angew. Chem. Int. Edit., 2123-2126.
15) H. Jobic, N. R. (2010). Unusual chain length dependance of the diffusion of n-alkanes in the metal-organic framework MIL-47(V): the blowgun effect. Chem-Eur J., 10337-10341.
16) J. A. Masson, M. V. (2014). Evaluating metal-organic frameworks for natural gas storage. Chem. Sci., 32-51.
17) James, S. J. (2003). Metal Organic Frameworks. Chem. Soc. Rev, 288.
18) Keskin, S. (2012). Recent Advances in Molecular. Koç University, Department of Chemical and Biological Engineering, 27.
19) L. Sarkisov, T. D. (2004). Molecular modeling of adsorption in novel nanoporous metal-organic materials. Mol. Phys. , 211.
20) Li, H. E. (1998). Establishing Microporosity in Open. J. Am. Chem. Soc.,, 120, 8571-8572.
21) Liu, J. K. (2011). Molecular Simulations and Theoretical. J. Phys. Chem. C,, 115, 12560-12566.
22) Loiseau, T. S. (2004). A Rationale for the Large Breathing of the Porous Aluminum Terephthalate. Chem.-Eur. J.,, 1382.

23) M. Eddaoudi, J. K. (2002). Systematic design of pore size and functionality in isoreticular MOFs and their application in methane storage. Science, 469-472.
24) N. J. Rosenbach, H. J. (2014). Diffusion of light hydrocarbons in flexible MIL-53(Cr) metal-organic framework: a combination of quasi elastic neutron scattering and molecular dynamics simulation. J. Phys. Chem. C, 3-14.
25) Park, K. S.-R. (2006). Exceptional Chemical and Thermal Stability of Zeolitic Imidazolate Frameworks. Proc. Natl. Acad. Sci. U. S. A, 10191.
26) Plimpton, S. (1995). Fast parallel algorithms for short range molecular dynamics. J. Comput. Phy., 1-19.
27) R. Babarao, Y. H. (2009). Molecular insight into adsorption and diffusion of alkane isomer mixtures in metal organic frameworks. J. Phys. Chem. B, 9129-9136.
28) S. Amirjalayer, M. T. (2006). Molecular dynamics simulation study of benzene diffusion in MOF-5: Importance of lattice dynamics. Angew Chem., 463-466.
29) S. Keskin, J. L. (2008). Testing accuracy of correlations for multicomponent mass transport of adsorbed gases in metal-organic frameworks: diffusion of H2/CH4 mixtures in CuBTC. Langmuir, 8254-61.
30) S. L. Mayo, B. D. (1990). DREIDING - A Generic force-field for molecular simulations. J. Phys. Chem., 8897-8909.
31) S. Rives, H. J. (2012). Diffusion of long chain n-alkanes in the metal-organic framework MIL-47(v): a combination of neutron scattering experiments and molecular dynamics simulations. Micropor. Mesopor. Mater., 259-265.
32) Sholl, A. I. (2005). Self-diffusion and transport diffusion of light gases in metal-organic framework materials assessed using molecular dynamics simulations. J. Phys. Chem. B, 15760-8.
33) Siepmann, M. G. (1998). Transferable potentials for phase equilibria. 1. United-atom description of n-alkanes. J. Phys. Chem. B, 2569-2577.
34) T. Duren, L. S. (2004). Design of new materials for methane storage. Langmuir, 2683-2689.
35) Tildesley, M. P. (1987). Computer simulations of liquids. New York: Oxford University Press.
36) Wheatley, R. E. (2008). Gas storage in nanoporous materials. Angew. Chem. -Int. Edit., 4966-4981.
37) Y. Peng, V. K. (2013). Methane storage in metal-organic frameworks: current records, surprise findings, and challenges. J. Am.Chem. Soc., 11887-11894.
38) Yaghi, J. R. (2009). The pervasive chemistry of metal-organic frameworks. Chem. Soc. Rev., 1213-1214.
39) Yaghi, O. M. (2003). Reticular Synthesis and the Design of New Materials. Nature,, 423, 705-714.
40) Yashonath, R. C. (1997). Estimation of error in the diffusion coefficient from molecular dynamics simulation. J. Phys. Chem. B, 5437-5445.
41) Zhou, S. M. (2010). Gas storage in porous metal-organic frameworks for clean energy applications. Chem. Commun., 44-53.